Ancillary Services and Dynamic Behavior of Inverters connected to the Low Voltage Grid

Markus Dietmannsberger, Detlef Schulz
Chair of Electrical Power Systems, Helmut Schmidt University / University of the Federal Armed Forces Hamburg
Holstenhofweg 85, 22043 Hamburg, Germany
Markus.Dietmannsberger@hsu-hh.de

***Abstract*—Small generators connected to the low voltage grid must be able to provide ancillary services in order to support system stability nowadays and in the future. Grid codes have been implemented that demand for load-frequency control and reactive power control. Together with anti-islanding-detection, these control algorithms mainly affect the dynamic behavior of the inverters in case of loss of mains. In this paper, an inverter model is presented that complies with the major grid codes. Islanding tests show new effects that arise because of the interaction between different control algorithms. Oscillating operating points may occur under special circumstances. This leads to further investigations on frequency dynamics. The additional benefit of rate-of-change-of-frequency (ROCOF) monitoring is numbered in a quantitative analysis and simulation. Not only steady state, but dynamic behavior is investigated with respect to the Non-Detection-Zone (NDZ). It is shown, that using frequency dynamics, scales down NDZs of passive anti-islanding methods significantly.**

***Index Terms*—anti-islanding; mains monitoring; inverter control; ancillary services; Non Detection Zone; rate of change of frequency; ROCOF**

I. Introduction

In the past, ancillary services have mainly been provided by big generators connected to the transmission grid. With an increasing share of distributed generation and the priority power feed from renewable energies, more and more of those big generators are replaced. In the future, ancillary services have to be provided by those distributed generators, too. This paper presents a model for a three phase inverter connected to the low voltage distribution grid. It consists of established components like power and current controller. In addition, several components were included, that ensure grid compatibility. Main components of the model are presented in section III. Focus was on ancillary services and anti islanding detection (AID) in particular. In sections IV and V, tests show the dynamic behavior of the model. With this model, further analysis can be done regarding dynamic behavior of inverters that comply with the standards of [1]. It will be shown, that the implementation of these standards may have unintentional effects on the behavior of the system during islanding conditions. In fact, there may be configurations that lead to oscillating operating points due to active and reactive power control. This can make AID ineffective. Technical reasons for this effect are explained and hence necessary changes in the standards are addressed.

There are several methods to identify islanding conditions. They can be split into three main groups: remote, local passive and local active. Categorizations can be found in [2], [3], [4]. Remote methods are based on some kind of communication between a central transmitter (e.g. alive signal) and multiple receivers (distributed generators). Passive methods rely on measuring grid parameters like voltage and frequency. Active methods try to perturb system parameters throughout their operation. Well established active AID methods are e.g. Active Frequency Drift (AFD) or Slip Mode Frequency Shift (SMS) [5]. They try to shift system frequency. When the inverter is connected to the grid, frequency is too stable to be shifted. After islanding occurred, AFD or SMS can easily shift islanding frequency. When exceeding upper or lower limits (47.5 or 51.5 Hz), the inverter trips and islanding is detected effectively. A comparison between different active methods can be found in [6]. Every (local) method has a so called Non-Detection-Zone where AID fails. Usually, size and form of NDZs are evaluated with parallel RLC loads [7], [8], [9]. Parallel RLC loads are assumed to be the worst case scenario for AID methods as they adapt to the inverter's current feed and changes in voltage and frequency are relatively small. As this is an accepted method in describing islanding events, the introduced model is simulated under these terms. Fig. 1 shows the NDZ of the SMS method. This method is state of the art, when active methods are used. There is virtually no NDZ for low quality factors.

Whereas a lot of investigation has been done on size and form of NDZs, those investigations mostly concentrate on steady state and barely take into account the dynamic behavior and the rate of changes of voltage and frequency in the event of islanding. Derived from the dynamic behaviors, the rate of change of frequency (ROCOF) is used and implemented in the model. Changes in frequency and in particular ROCOF have been under investigation for AID [2]. In [10], a detailed investigation on different settings of ROCOF relays is presented. Whereas in [10], the different implementations are compared regarding false tripping, this paper deals with the impact of the ROCOF method on the NDZ.

By applying a simple ROCOF method using the PLL frequency, quantitative results on changes of the NDZ can be

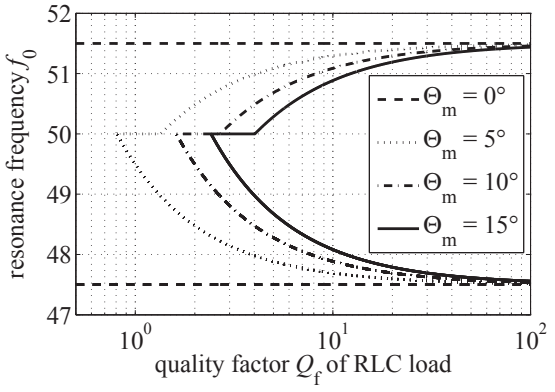

Fig. 1. Non-Detection-Zone (NDZ) of the SMS method; for strong SMS parameters (big Θ_m), there is no NDZ for low quality factors

presented for inverters with respect to low voltage grid codes. Once again, the findings of this paper are used to address necessary changes in the standards.

II. Ancillary Services and Anti Islanding Detection According to Low Voltage Grid Codes

Smaller generators connected to the distribution grid have to provide ancillary services in the future. These services mainly include: general operation management (including AID), load-frequency control, voltage and reactive power control and black starting capability. To ensure participation in ancillary services in the low voltage grid, new guidelines concerning generators connected to the low-voltage distribution network were published, e.g. in the VDE AR N 4105 in Germany in 2011 [1]. In this standard, technical requirements for the connection to and parallel operation with low-voltage distribution networks are introduced. The standards, that are relevant for further research in this paper, are presented briefly. Therefore, [1] is taken as a descriptive example, but can also be used for other countries.

A. Voltage and Frequency Limits

All generators have to disconnect from the grid when the actual voltage drops below 0.8 V_g or exceeds 1.15 V_g. If a 10-min mean value of 1.10 V_g is exceeded, the generator must trip as well. This ensures that power quality is kept according to EN 50160. Voltage measurement shall be done by calculating the RMS value for a half-period of nominal grid frequency f_g. Generators have to measure voltages of all phases that they inject power into. Hence for a three phase inverter like in this paper, all three voltages L1-N, L2-N and L3-N have to be monitored. Violation of voltage limits have to be logically linked OR, i.e. if only one voltage out of three is outside the allowed range, generators have to disconnect.

In Europe, nominal grid frequency $f_{g,n}$ is 50 Hz. In the past, there have been several limits for generators in the low voltage grid regarding frequency changes. The grid code DIN V VDE 0126-1-1 [11] introduced limits of 47.5 Hz and 50.2 Hz

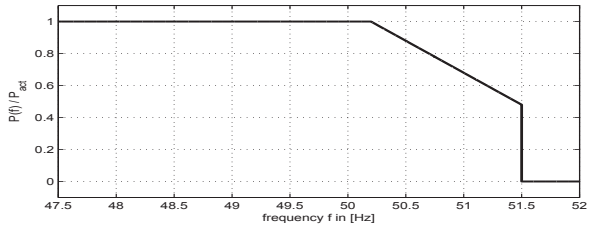

Fig. 2. Frequency dependent active power reduction according to [1]

in 2006. This quite low upper limit lead to the so called "50.2 Hz problem". This could evoke major dynamic impacts if all generators in the low voltage grid (mainly photovoltaic inverters) trip at the same time, leading to a major imbalance in production and consumption of electric energy. Therefore, frequency limits have been changed to 47.5 Hz and 51.5 Hz. These values have been transferred into [1], which replaced [11] in 2012.

B. Reduction of Active Power in case of over frequency

An imbalance of production and consumption of electric energy in the system leads to frequency changes and deviations from 50 Hz. This frequency change activates the primary power control of big generators in order to bring back frequency to 50 Hz. According to [1], generators in low voltage grids must provide active power reduction in case of over frequency as well. With frequency exceeding 50.2 Hz, active power P_{act} of the actual operating point has to be reduced by 40 %/Hz. When system frequency exceeds 51.5 Hz, generators must disconnect from the grid. If frequency drops below 50.2 Hz again, the generators can increase their active power by 10 % of P_n per minute if possible. Equation (1) represents the standard of [1] and Fig. 2 illustrates the different sectors of active power control.

$$P(f) = P_{act} \cdot (1 - 0.4 \cdot (f_g - 50.2\ \text{Hz})) \quad \text{for } 50.2\ \text{Hz} \leq f_g \leq 51.5\ \text{Hz} \tag{1}$$

When generators are not able to implement a behavior according to this standard, manufacturers have to ensure that generators trip at a random frequency between 50.2 and 51.5 Hz, equally distributed over all produced inverters.

C. Injection of Reactive Power

Increasing generation in low voltage grids leads to an increase of voltage due to the injected current. That is why generators have to be able to provide negative (and positive) reactive power in most of their operating points. According to [1], all generators up to a nominal power of 13.8 kVA have to be able to operate within the range of $cos\varphi = 0.95$ under-excited and $cos\varphi = 0.95$ over-excited if the level of active power P_{act} exceeds 20 % of P_n. The curve of reactive power is prescribed by the network operator. If there are no further prescriptions, the inverter has to follow the standard curve shown in Fig. 3. The mathematical representation is

$$cos\varphi = min(1, 1.05 - 0.1 \cdot \frac{P_{act}}{P_n}) \tag{2}$$

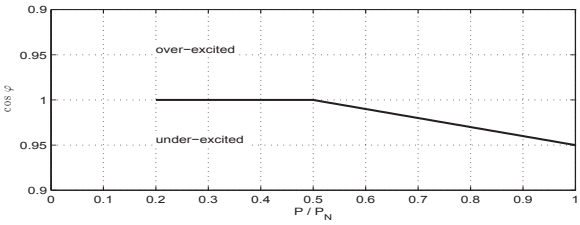

Fig. 3. Power factor $cos\varphi(P)$ for generators with $S_{\max} \leq$ 13,8 kVA according to [1]

D. Anti-Islanding Protection

Implementation of anti-islanding (AI) protection according to [1] has to be differentiated between single-phase and three-phase inverters and directly coupled generators (e.g. synchronous machines). For directly coupled generators and single-phase inverters, passive methods like three-phase voltage monitoring is sufficient. Three-phase inverters have to use active methods, like e.g. active frequency drift. AI detection has to be implemented in a "grid and plant protection device" (also called bidirectional safety interface, BISI). Islanding has to be detected within five seconds. In this paper, a model for a three phase inverter is presented. No active AID method has been implemented in order to scrutinize the behavior of passive methods in case of islanding and the real size and form of Non-Detection-Zones (NDZ) when dynamic effects are considered. The results are shown in sections IV and V.

III. Matlab Simulink Model

A. General Modeling Approach

Fig. 4 shows the general overview of the applied model that has been used for the simulation. It consists of a constant voltage source at the DC side, the inverter model, a measuring point at the point of common coupling (PCC), a parallel RLC load for each phase, a three phase breaker and three controllable voltage sources, one for each phase. The breaker can be used to set the system in islanding mode (see section IV and V). The details of the components and general settings can be found in Table I. For the inverter, a two level, three phase model of MOSFETs is used. Parameters $R_{\rm on}$, $R_{\rm d}$, and $V_{\rm d}$ are set according to [12]. Their relevance is limited as there is no investigation on power losses at the moment. Triggering of the MOSFETs is realized with a PWM. The PWM signals are calculated via the modulation signal $m_{\rm abc}$ that is transformed from *dq*-frame to *abc*-frame.
As we investigate dynamic grid behavior especially in islanding situations, the DC side of the inverter can be simplified with a constant voltage source. The dynamic behavior that is important for an evaluation of islanding protection should be independent of fluctuations in power production on the DC side (e.g. radiation) due to the short time window ($T_{\rm sim} \leq 5$ s). Most important for the model behavior are the applied control algorithms shown in the following.

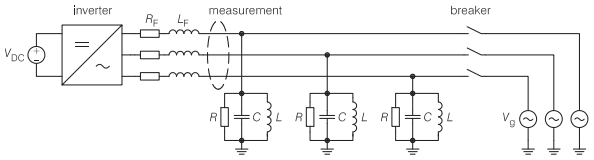

Fig. 4. Matlab / Simulink Model: General Overview

TABLE I
Components and Settings

Symbol	Description	Value
$V_{\rm g}$	Nominal grid voltage	230 V
$f_{\rm g}$	Nominal grid frequency	50 Hz
$V_{\rm d}$	Internal diode forward voltage (Mosfet)	1 V
$R_{\rm on}$	Internal diode forward resistance (Mosfet)	0.88 mΩ
$f_{\rm PWM}$	PWM frequency	5 kHz
$V_{\rm DC}$	DC voltage	1000 V
$L_{\rm F}$	Filter inductance	5 mH
$R_{\rm F}$	Filter resistance	0.75 mΩ

B. Modeling of Current Control

The overall control of the inverter is implemented in a dq-frame, as shown in Fig. 5. This provides some advantages over abc-frame. First, d- and q-components are DC variables which result in an easy controllability. Thus we can use simple PI compensators in the control loop. Furthermore active and reactive power can be controlled almost independently from each other (except for dynamic coupling). Transforming all measured variables (voltages and currents) into dq-frame, calculating the control outputs and finally transforming them back into abc-frame leads to a simple and straight-forward control algorithm.

Regarding the current control in Fig. 5, the state variable $i_{\rm d}$ ($i_{\rm q}$) is subtracted from the reference input $i_{\rm d,ref}$ ($i_{\rm q,ref}$). The error $e_{\rm d}$ ($e_{\rm q}$) is the input for the PI compensator. The resulting control input $V_{\rm d}$ ($V_{\rm q}$) is then calculated from the actuating variable $u_{\rm d}$ ($u_{\rm q}$) and the two feed forward signals $V_{\rm g,d}$ ($V_{\rm g,q}$) and $ff_{\rm q}$ ($ff_{\rm d}$). Finally the modulation signals $m_{\rm d}$ and $m_{\rm q}$ are derived and transformed to $m_{\rm abc}$.

The control loops of Fig. 5 are based on the assumption of a steady state operation and a constant frequency ω_0 which results in the following equations that are developed and derived in detail in [12]:

$$0 = L \cdot \frac{di_{\rm d}}{dt} - L_{\rm F} \cdot \omega_0 \cdot i_{\rm q} + R_{\rm F} \cdot i_{\rm d} - V_{\rm d}(t) + V_{\rm g,d} \qquad (3)$$

$$0 = L \cdot \frac{di_{\rm q}}{dt} - L_{\rm F} \cdot \omega_0 \cdot i_{\rm d} + R_{\rm F} \cdot i_{\rm q} - V_{\rm q}(t) + V_{\rm g,q} \qquad (4)$$

Equations (3) and (4) indicate the dynamic coupling between the *d*- and *q*- components due to the filter inductance $L_{\rm F}$. Therefore a dynamic decoupling is in place that calculates feed forward signals $ff_{\rm d}$ and $ff_{\rm q}$. Further feed forward signals $V_{\rm g,d}$

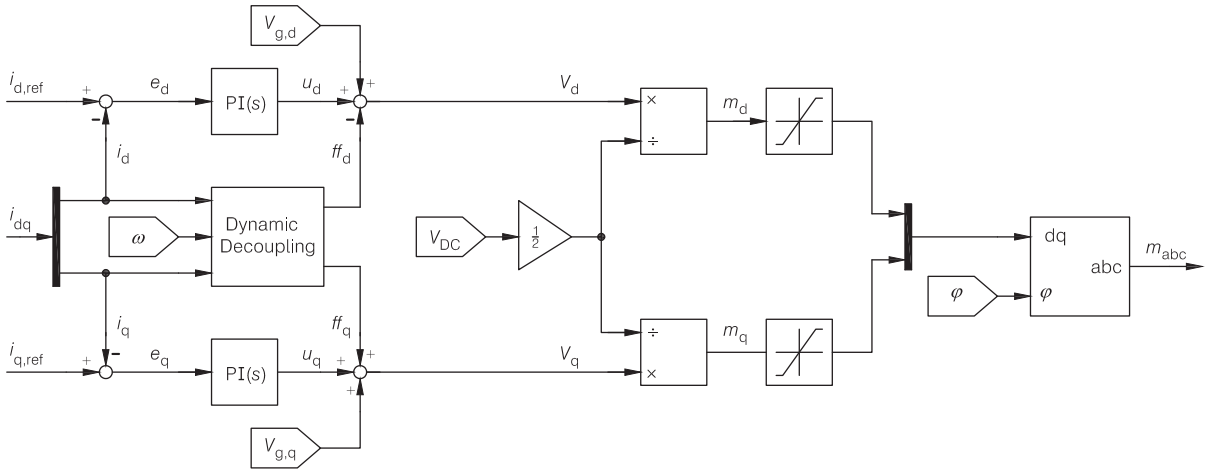

Fig. 5. Design of the current controller in dq-frame

and $V_{\mathrm{g,q}}$ are implemented in order to provide fast reaction to changes in grid voltage.

C. Modeling of Active and Reactive Power Control

Implementing the control algorithms for active and reactive power once again shows the advantages of the dq-frame. From [12] it applies

$$P(t) = \frac{3}{2} \cdot [V_{\mathrm{g,d}}(t) \cdot i_{\mathrm{d}}(t) + V_{\mathrm{g,q}}(t) \cdot i_{\mathrm{q}}(t)] \tag{5}$$

$$Q(t) = -\frac{3}{2} \cdot [V_{\mathrm{g,d}}(t) \cdot i_{\mathrm{q}}(t) + V_{\mathrm{g,q}}(t) \cdot i_{\mathrm{d}}(t)] \tag{6}$$

With the phase-locked-loop controlling the q-component of the grid voltage ($V_{\mathrm{g,q}}$) to zero in a steady state mode, the calculation of active and reactive power can be simplified [12]:

$$P(t) = \frac{3}{2} \cdot V_{\mathrm{g,d}}(t) \cdot i_{\mathrm{d}}(t) \tag{7}$$

$$Q(t) = -\frac{3}{2} \cdot V_{\mathrm{g,d}}(t) \cdot i_{\mathrm{q}}(t) \tag{8}$$

Resulting in a linear relationship between $P(t)$ and i_{d} as well as $Q(t)$ and i_{q}. Because of this, modeling the control for active and reactive power due to the standards for generators connected to the low voltage grid in section II can be done straight forward. Fig. 6 shows the setting of the power controller. The nominal values for normal operation are given by the set of standards introduced in section II and mainly consists of $P(f)$ and $Q(P)$ control. Tripping of the inverter sets P_{ref} and Q_{ref} to zero.

D. Modeling of P(f)-control and Q(P)-control

As explained in section II, the main aspect of grid code compatibility in this paper is about control of active and reactive power. Fig. 7 shows the implementation of the frequency dependent active power reduction, $P(f)$. As long as the measured frequency is below 50.2 Hz, the active power fed into the grid remains unchanged. When exceeding this limit, the actual power value is stored via a sample-and-hold block. The curve of Fig. 2 shows, how big the reduction of

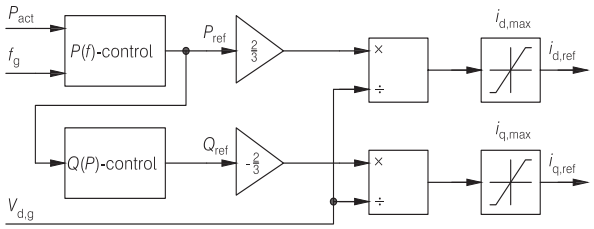

Fig. 6. Design of the power controller in dq-frame

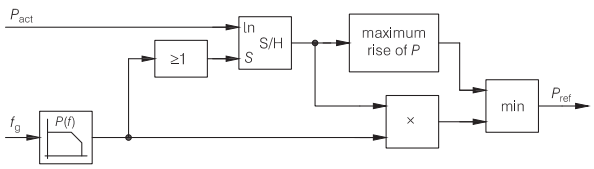

Fig. 7. $P(f)$ control

active power must be. This is finally set as a reference value P_{ref} for the overall power control. This leads to a reduction of injected power within a few milliseconds, quick enough to ensure power system stability in reality.

Fig. 8 shows the algorithm for the $Q(P)$-control. The active power P_{ref} is compared to the nominal power of the inverter P_{n}. The curve of Fig. 3 determines whether the inverter has to provide reactive power. Via the trigonometric functions tan and cos^{-1}, the correct reactive power Q_{PV} is computed:

$$Q_{\mathrm{ref}} = -P_{\mathrm{ref}} \cdot \sqrt{\frac{1}{cos^2\varphi} - 1} = -P_{\mathrm{ref}} \cdot tan\varphi \tag{9}$$

Finally, Q_{ref} is provided as reference value for the overall reactive power control.

E. Modeling of AID

Detection of islanding is mainly based on exceeding upper and lower limits for frequency and voltage. From the standards

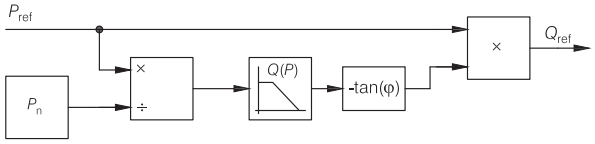

Fig. 8. $Q(P)$ control

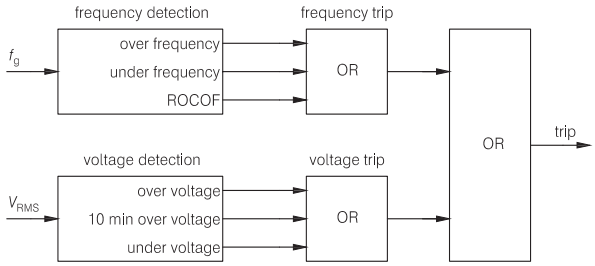

Fig. 9. AID algorithm

introduced in section II one can derive for the distinction of AID:

- A violation of frequency limits ($f_\mathrm{g} < 47.5$ Hz or $f_\mathrm{g} > 51.5$ Hz) always indicates islanding. Thus frequency detection is directly connected to islanding protection.
- In addition to the violation of frequency limits, a monitoring for the rate of change of frequency (ROCOF) is implemented. If the ROCOF value exceeds a certain limit, tripping is triggered (details see section V).
- Exceeding the upper or lower voltage limits results in triggering AID. This can be split up into over-voltage of the 10 min mean value ($1.10\ V_\mathrm{g,n}$), over-voltage of actual voltage ($1.15\ V_\mathrm{g,n}$) and under-voltage of actual voltage ($0.8\ V_\mathrm{g,n}$).

Fig. 9 shows a summary of the implementation of islanding protection. According to [1], all triggers are logically linked OR. Over-voltage and under-voltage limits are applied to all three phases.

IV. Alterinating Operating Points in Islanding due to Low Voltage Grid Codes

Islanding can be simulated by opening the circuit breaker. The loss of mains leads to new operating points depending on active and reactive power of the inverter and the values for the RLC loads. These operating points have a defined voltage (V_OP) and frequency (f_OP) which can be calculated by setting up the balance for active and reactive power. With f_res and Q_f being the resonance frequency and quality factor of the RLC load respectively. P_OP is the active and Q_OP the reactive power of the inverter after islanding:

$$f_\mathrm{OP} = \frac{1}{2} \cdot \left(-\frac{f_\mathrm{res} \cdot Q_\mathrm{OP}}{P_\mathrm{OP} \cdot Q_\mathrm{f}} + \sqrt{\left(\frac{f_\mathrm{res} \cdot Q_\mathrm{OP}}{P_\mathrm{OP} \cdot Q_\mathrm{f}} \right)^2 + 4 \cdot f_\mathrm{res}^2} \right) \tag{10}$$

$$V_\mathrm{OP} = \sqrt{\frac{1}{3} \cdot P_\mathrm{OP} \cdot R} \tag{11}$$

$$Q_\mathrm{f} = R \cdot \sqrt{\frac{C}{L}} \quad , \quad f_\mathrm{res} = \frac{1}{2 \cdot \pi \cdot \sqrt{L \cdot C}} \tag{12}$$

If the grid codes of section II are implemented, P_OP is sensitive to f_OP and Q_OP is sensitive to P_OP which depends on f_OP again. This hypothesizes, that there might be oscillating operating points with different frequencies. The model presented in this paper can be used to verify this hypothesis.

Therefore, the values of Table II are set up. Fig. 10 shows the result. At $t_1 = 0.05$ s the inverter starts injecting 6 kW of active power and -855 var of reactive power into the grid. The system is stabilized within a few milliseconds. The equivalent current components i_d and i_q are shown in the middle and lower part of the diagram respectively. At $t_2 = 0.1$ s mains is disconnected. Due to (10) the new operating point in islanding mode would be at $f_\mathrm{OP} = 51.8$ Hz. Normally, islanding frequency would now rise and asymptotically converge towards this value. But when 50.2 Hz is exceeded at about 0.13 s, the $P(f)$ control is activated and reduces the actual active power of the inverter. This leads to a reduction of reactive power because of the $Q(P)$ control. At $t_3 = 0.171$ s active power is reduced underneath 0.5 P_n. At this point, the inverter doesn't provide reactive power anymore ($Q_\mathrm{OP} = 0$). This makes the system frequency decrease. It would move back to 50 Hz which is the initial resonance frequency of the RLC load. But at $t_4 = 0.188$ s active power exceeds 0.5 P_n and immediately reactive power is provided again. System frequency is rising and the oscillation starts again. This can be observed in Fig. 10. The oscillation depends on the following dynamic properties of the system.

- Resonance frequency of the RLC load: the resonance frequency of the RLC load is the frequency, the system would move to, if the inverter didn't provide reactive power. This is the case, when active power is underneath 0.5 P_n.
- Quality factor of the RLC load: the higher the quality factor, the more reactive power is needed for the same amount of frequency change, see (10). In case of a high quality factor, the system is more likely to be stabilized in oscillation.
- Time constant of $P(f)$ control: A reduction of active power leads to decreasing system voltage, thus affecting reactive power and system frequency as well. But this secondary effect is rather small.
- Time constant of $Q(P)$ control: Reactive power directly affects islanding frequency, see (10). Thus the time con-

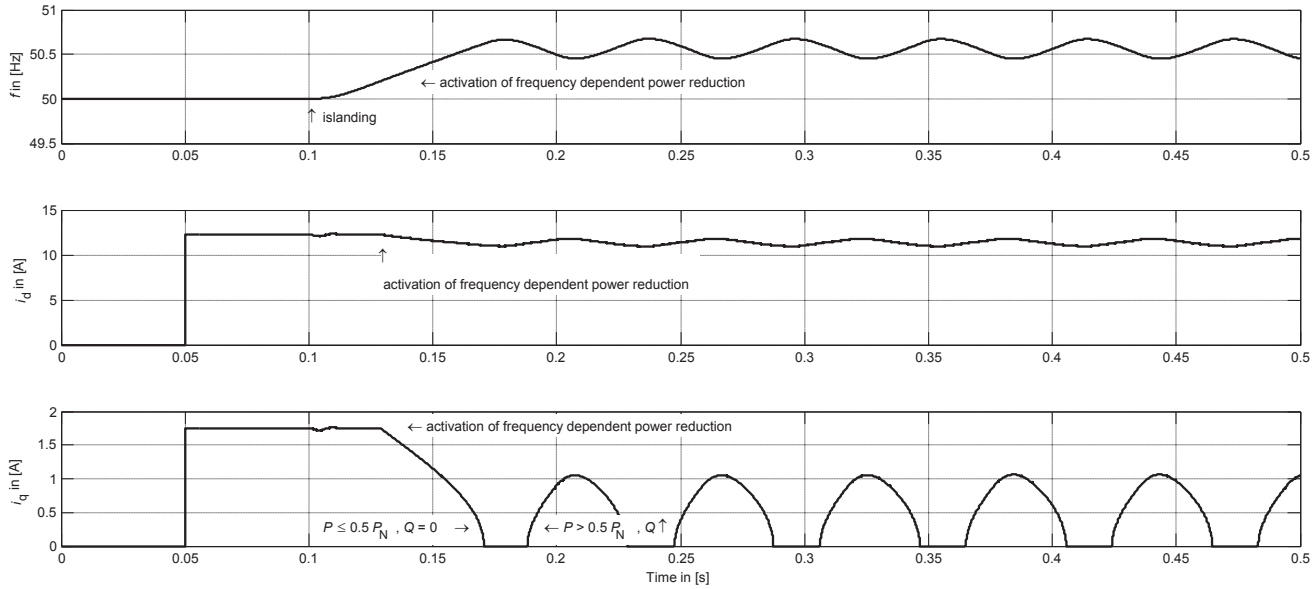

Fig. 10. Oscillating operation points due to interactions between different control algorithms; top: frequency curve; center: i_d curve as an indicator for active power; bottom: i_q curve as an indicator for reactive power

stants of the change of reactive power needs to be small enough to stop the rise of frequency before it exceeds the upper limit, 51.5 Hz.

- Derivative time constant of PLL: The measured frequency for AID and power control comes from the PLL. Normally, PLLs have a rate limiter for the maximum rate of change of frequency (ROCOF). The bigger this value, the faster the inverter can detect changes in system frequency. As the inverter is the only source in an island, frequency changes can only be evoked by its current injection. Due to this, a slow PLL results in slow changes of the islanding frequency, and vice versa.

The special dynamic behavior that evokes the oscillating operating points after loss of mains strongly depends on the interaction between the dynamic behavior of the PLL and the $Q(P)$ control.

Taking the above considerations leads to an area of operating points, where the oscillations can occur: Active power has to drop below $0.5\ P_\mathrm{n}$ in order to set $Q = 0$. Thus, the closer P_act is to $0.5\ P_\mathrm{n}$, the quicker this point is reached. Within the rise time of islanding frequency from 50.2 Hz to 51.5 Hz, the total power reduction (active and thus reactive) has to be applied. The resulting time windows in a first approximation is:

$$\frac{(51.5 - 50.2)\ \mathrm{Hz}}{df_\mathrm{PLL,max}} = \frac{1.3\ \mathrm{Hz}}{10\ \frac{\mathrm{Hz}}{\mathrm{s}}} = 0.13\ \mathrm{s} \tag{13}$$

As long as

$$T_\mathrm{P(f)} + T_\mathrm{Q(P)} > \frac{1.3\ \mathrm{Hz}}{df_\mathrm{PLL,max}} \tag{14}$$

no oscillations can occur as power control is always too slow to respond to frequency changes. In the simulation shown in Fig. 10, $T_\mathrm{P(f)} + T_\mathrm{Q(P)} = 2\ \mathrm{ms} < 0.13\ \mathrm{s}$. In real inverters, time constants of $Q(P)$ control normally are in the range of a few seconds whereas PLLs are much quicker. Thus, in islanding, the new operating frequency will be reached very quickly so the reactive power can't be reduced on time and AID is effective.

TABLE II
SIMULATION PARAMETERS FOR OSCILLATION

Symbol	Description	Value
P_n	Nominal Power of the inverter	10 kW
P_inv	Active Power of the inverter before islanding	6 kW
Q_inv	Reactive Power of the inverter before islanding	-855 var
cos_φ	Maximum cosφ the inverter has to provide according to [1]	0.95
Q_f	Quality factor of the RLC load	2
f_res	Resonance frequency of the RLC load	50 Hz
f_OP	New operating frequency in islanding mode without $P(f)$ and $Q(P)$ control	51.8 Hz
τ_i	Time constant for current controller (d- and q-component) and for P- and Q-control	1 ms
$df_\mathrm{PLL,max}$	Maximum Rate of Change of Frequency (ROCOF) of the Phase Locked Loop (PLL)	10 Hz/s

V. DYNAMIC FREQUENCY BEHAVIOR IN CASE OF ISLANDING

Changes in frequency and in particular ROCOF can be used for AID [2], [3]. Due to [1], new islanding protection devices have been developed, that already are able to use ROCOF as a detection method. Nevertheless the additional benefit of ROCOF for a decreasing size of the NDZ has not yet been quantified.

Therefore it needs to be identified, how frequency changes happen in the case of islanding. The setup for the following simulation can be found in Table III. In this case, an operating point with no reactive power is used. Because of this, f_{res} and f_{OP} are the same, which makes things easier to understand. In the event of islanding, the frequency will change from nominal value (50 Hz) to f_{res}, because there is the balance of active and reactive power (resonance means zero reactive power consumption of the parallel RLC load). Depending on the quality factor, the frequency change will be quicker or slower. $df_{\mathrm{PLL,max}}$ limits the changes. Simulations are done according to the parameters of Table III. For each configuration, ROCOF is recorded and finally the maximum value is investigated. An exemplary frequency curve over time can be found in Fig. 11 (left).

Fig. 11 (right) shows, the bigger the delta between nominal frequency and resonance frequency, the faster the frequency changes. In case of big deltas, $df_{\mathrm{PLL,max}}$ limits the values. This means, that there cannot be any changes in frequency that are faster than the maximum ROCOF parameter in the PLL. Fig. 11 (right) also shows the effect of the quality factor. The higher the quality factor, the faster the frequency changes. On the assumption of a delta between nominal and resonance frequency of 0.2 Hz, significant values for ROCOF (more than 2 Hz/s) already occur for quality factors higher than 0.5. As active and reactive power feed does not change, the time constants of the current and power controller do not affect the behavior.

Even for small deviations from nominal grid frequency $f_{\mathrm{g,n}}$ the values increase quickly. The findings of Fig. 11 can be used to quantify the effects on size and form of NDZs. Normally, frequency deviations in Europe are in the range of less than 10 mHz/s [13]. Even in smaller networks like in Ireland, grids face ROCOFs of about 0.5 Hz/s [14]. This means, that even by taking a safety margin, a limit of about 2 Hz/s would be possible as an AID limit. Commercial BISI devices can provide ROCOF limits from 0.05 to 10 Hz/s.

The ROCOF minima in Fig. 11 are not located at the nominal frequency of 50 Hz. This is due to the filter inductance of the inverter. It slightly shifts the resonance of the parallel RLC load. This effect decreases with increasing quality factor, see Fig. 11. The resonance becomes stronger in comparison to the filter inductance.

Taking a look at Fig. 12 reveals the reduction of the NDZ by taking into account the dynamic behavior of the islanded system. A limit of 2 Hz/s as a maximum ROCOF results in an NDZ that has less than 7.5 % the size of the original NDZ (upper limit: $f_{\mathrm{res}} = 51.5$ Hz, lower limit: $f_{\mathrm{res}} = 47.5$ Hz). Islanding detection is effective with all relevant values for Q_{f} and at resonance frequencies below 49.95 Hz and above 50.30 Hz. Values for Q_{f} smaller than 0.5 are not shown in this diagram because in this range, the inductive part of the RLC load becomes bigger than 850 mH, see (12), and thus this is not relevant for real conditions. In fact, the ROCOF depends on the absolute value of reactive power imbalance during frequency changes.

TABLE III
VALUES FOR DYNAMIC FREQUENCY ANALYSIS

Symbol	Description	Value
P_{inv}	Active Power before islanding	4 kW
Q_{f}	Quality factor of the RLC load	0.5...10
f_{res}	Resonance frequency of the RLC load	49.5...50.5 Hz
$df_{\mathrm{PLL,max}}$	ROCOF of the PLL	5/10/20 Hz/s

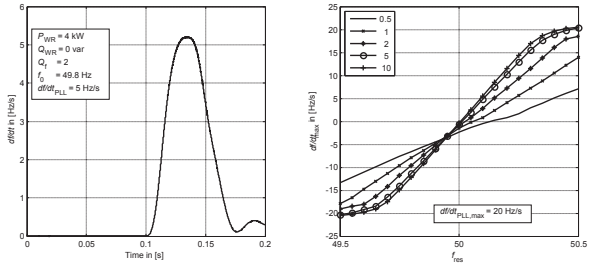

Fig. 11. Frequency dynamics in case of Islanding; left: $\frac{df}{dt}$ curve after islanding event with $\frac{df}{dt}_{\mathrm{PLL,max}} = 20\ \frac{\mathrm{Hz}}{s}$; right: frequency changes dependent on Q_{f} and f_{res} and

Active methods have weaknesses when applied in grids with high quality factors [15]. As the ROCOF method is effective in exactly those cases, the combination of the two could increase effectiveness of overall AID. In addition, negative influence of active AID-methods (permanent disturbance of system frequency, increased amount of harmonic distortion, danger of system instability with high shares of inverters, etc.) can be reduced by weakening active methods (choosing a smaller Θ_{m}) and the amount of frequency shifting. In fact, this enables the inverter to discriminate between *detection* and *shutdown* of an island. As long as system frequency stays within the tolerable limits, the system can stay alive and can possibly be reconnected when grid connection is reestablished. The requirements for this event (phasing and balance of voltage and frequency) can be investigated in future research.

VI. CONCLUSION

In this paper, the main aspects of ancillary services in low voltage grid codes are introduced and the major impacts for dynamic behavior of inverters have been highlighted. In addition, the connection between active and reactive power control and AID was elaborated.

In section III, a new model for an inverter that includes an effective passive anti-islanding-detection (AID) was presented. In addition the model is according to (German) grid standards [1] i.e. providing ancillary services like active

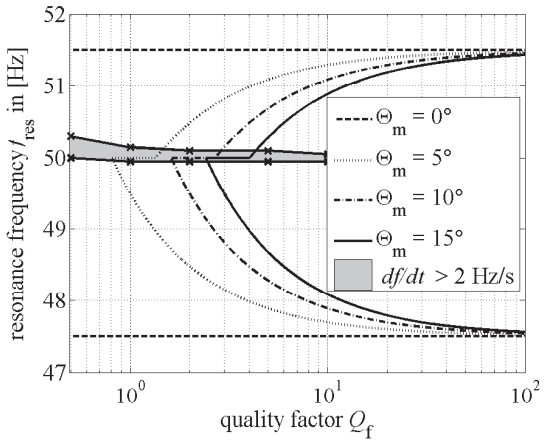

Fig. 12. resulting NDZ for ROCOF method with a limit of 2 $\frac{\text{Hz}}{s}$ (grey area); compared to the SMS method

power reduction due to over-frequency ($P(f)$-control) and reactive power supply ($Q(P)$-control).

The model was applied to investigate interactions between ancillary services and the effectiveness of AID in section IV. Therefore, a RLC load was connected and the system was islanded. It was shown, that the implemented control algorithms can result in a stable oscillation that makes the inverter operate in forbidden islanding. This effect depends on the quality factor and resonance frequency of the load that is connected to the inverter and on the time constants of the current and power control algorithms and the PLL. To date, almost no standards regarding time constants are set in [1]. Theoretically this allows inverters to show this effect. The results of this paper make a contribution to the fact, that more precise standards regarding dynamic behavior must be introduced in future revisions of [1].

Section V showed, that dynamic frequency changes in the event of islanding can support AID and help reducing Non-Detection-Zones (NDZ) significantly. This can be achieved by implementing monitoring of the rate of change of frequency (ROCOF). A detailed analysis on the relevant parameters has been executed. Depending on resonance frequency of the parallel RLC load and its quality factor, frequency changes fast enough to detect unintentional islanding with a reasonable threshold of 2 Hz/s. This reduces the size of the NDZ to less than 7.5 %. The applied analysis in this paper can help establish more adequate grid standards because the limits of the ROCOF method on size and form of the NDZ have been quantified. With respect to AID, passive detection methods could be applied more effectively.

REFERENCES

[1] Verband der Elektrotechnik Elektronik Informationstechnik e.V., "Generators connected to the Low-Voltage Distribution Network." no. VDE-AR-N 4105:2011-08, 2011.

[2] W. Bower and M. Ropp, "Evaluation of islanding detection methods for utility-interactive inverters in photovoltaic systems," *Sandia Report SAND*, no. November, 2002.

[3] P. Mahat, Z. Chen, and B. Bak-jensen, "Review of Islanding Detection Methods for Distributed Generation," no. April, pp. 2743–2748, 2008.

[4] D. Schulz, *Grid Integration of Wind Energy Systems. In German: Integration von Windkraftanlagen in Energieversorgungsnetze Stand der Technik und Perspektiven für die dezentrale Stromerzeugung*. Berlin und Offenbach: VDE Verlag GmbH, 2006.

[5] M. Ropp, M. Begovic, and A. Rohatgi, "Analysis and performance assessment of the active frequency drift method of islanding prevention," *IEEE Transactions on Energy Conversion*, vol. 14, no. 3, pp. 810–816, 1999.

[6] F. Liu, Y. Zhang, M. Xue, X. Lin, and Y. Kang, "Investigation and evaluation of active frequency drifting methods in multiple grid-connected inverters," *IET Power Electronics*, vol. 5, no. 4, p. 485, 2012.

[7] A. Ellis, S. Gonzalez, Y. Miyamoto, M. Ropp, D. Schutz, and T. Sato, "Comparative analysis of anti-islanding requirements and test procedures in the United States and Japan," in *2013 IEEE 39th Photovoltaic Specialists Conference (PVSC)*. IEEE, Jun. 2013, pp. 3134–3140.

[8] A. Woyte, R. Belmans, and J. Nijs, "Testing the islanding protection function of photovoltaic inverters," *IEEE Transactions on Energy Conversion*, vol. 18, no. 1, pp. 157–162, Mar. 2003.

[9] L. Lopes, "Analysis and comparison of islanding detection methods using a new load parameter space," in *30th Annual Conference of IEEE Industrial Electronics Society, 2004. IECON 2004*, vol. 2. IEEE, 2004, pp. 1172–1177.

[10] C. Ten and P. Crossley, "Evaluation of ROCOF relay performances on networks with distributed generation," *IET 9th International Conference on Developments in Power Systems Protection (DPSP 2008)*, vol. 2008, pp. 522–527, 2008.

[11] Verband der Elektrotechnik Elektronik Informationstechnik e.V, "Automated disconnection Device between a Generator and the Low-Voltage Grid." no. DIN VDE V 0126-1-1:2013-08, 2013.

[12] A. Yazdani and R. Iravani, *Voltage-Sourced Converters in Power Systems: Modeling, Control and Applications*. Hoboken, New Jersey: John Wiley & Sons Inc., 2010.

[13] Entso-E and Eurelectric, "Deterministic frequency deviations root causes and proposals for potential solutions," *EU Energy*, no. December, 2011.

[14] EIRGRID, "Ensuring a Secure , Reliable and Efficient Power System in a Changing Environment June 2011," EIRGRID, Tech. Rep. June, 2011.

[15] R. Reedy, K. Davis, D. Click, M. Ropp, and A. Shaffer, "Power line carrier permissive as a simple and safe method of enabling inverter ride-through operation of distributed grid-tied photovoltaic systems," in *2011 IEEE International Symposium on Power Line Communications and Its Applications*. IEEE, Apr. 2011, pp. 209–212.